

Feldkamp-type image reconstruction from equiangular data

Ben Wang^a, Hong Liu^b, Shiyong Zhao^c and Ge Wang^d

^a*Department of Elec. and Comp. Engineering, Beijing Union University, Beijing 100101, China*
E-mail: wbt1@publica.bj.cninfo.net

^b*University of Oklahoma, 202 west Boyd, Room 219, Norman, OK 73019, USA*
E-mail: liu@ou.edu

^c*Department of Math. & Comp. Science, University of Missouri at St. Louis, St. Louis, MO 63121, USA*

E-mail: zhao@arch.umsl.edu

^d*Department of Radiology, University of Iowa, Iowa City, Iowa 52242, USA*
E-mail: ge-wang@uiowa.edu

Abstract. The cone-beam approach for image reconstruction attracts an increasing attention in various applications, especially medical imaging. Previously, the traditional practical cone-beam reconstruction method, the Feldkamp algorithm, was generalized into the case of spiral/helical scanning loci with equispacial cone-beam projection data. In this paper, we formulated the generalized Feldkamp algorithm in the case of equiangular cone-beam projection data, and performed numerical simulation to evaluate the image quality. Because medical multi-slice/cone-beam CT scanners typically use equiangular projection data, our new formula may be useful in this area as a framework for further refinement and a benchmark for comparison.

Keywords: Computed tomography (CT), cone-beam geometry, Feldkamp-type reconstruction, medical imaging

1. Introduction

Recently, spiral/helical CT began a transition from fan-beam to cone-beam geometry with the introduction of multi-slice systems [1,2]. These narrow-angle cone-beam spiral CT scanners, also referred to as multi-slice or multi-row detector scanners, are already commercially available. Cone-beam spiral CT uses a 2D-detector array allows larger scanning range in shorter time with higher image resolution, and has important medical and other applications.

Despite progress in exact cone-beam reconstruction [3,4], approximate cone-beam algorithms, especially Feldkamp-type algorithms, remain valuable in practice [5–8]. The three advantages of approximate cone-beam reconstruction are as follows. First, incomplete scanning loci can be used with approximate reconstruction. The completeness condition for exact reconstruction requires that there exist at least a source position on any plane intersecting an object to be reconstructed. This condition may not be satisfied in many cases of X-ray CT. Second, computational efficiency of approximate reconstruction is high. Typically, approximate reconstruction involves less raw data than exact reconstruction. Also, the computational structure of approximate reconstruction is straightforward, highly parallel, hardware-supported,

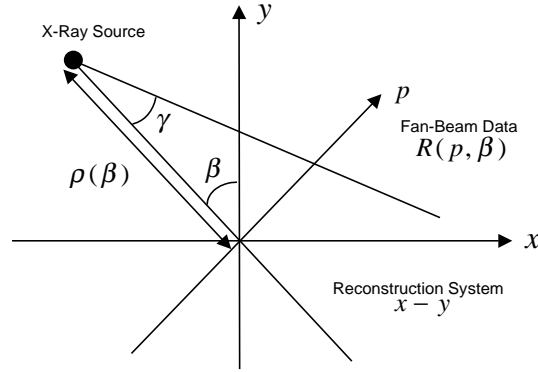


Fig. 1. Geometry of equispacial fan-beam reconstruction

and particularly fast for reconstruction of a small region of interest (ROI). Third, image noise, blurring/ringing artifacts may be less with approximate reconstruction. With the direct Fourier method [3], it was found that the exact reconstruction produced more ringing as compared to the Feldkamp method. It appears that this type of ringing is inherent to all exact cone-beam reconstruction formulas that take the second derivative of data. Furthermore, Feldkamp-type algorithms are widely used to benchmark the performance of new cone-beam algorithms.

Traditionally, Feldkamp-type cone-beam reconstruction algorithms were formulated for equispacial cone-beam projection data [5–8]. However, in medical cone-beam X-ray CT, projection data are typically represented in an equiangular format. Although the transformation from equiangular data to equispacial data does not represent any major challenge, the involved data interpolation procedure would compromise the spatial resolution of reconstructed images. In this paper, we represent a generalized Feldkamp image reconstruction formula that handles equiangular cone-beam projection data directly, and perform a numerical simulation study to evaluate the new formula using the 3D Shepp and Logan phantom.

2. Generalized Feldkamp reconstruction in the equispacial case

Feldkamp et al. adapted the conventional equispacial fan-beam algorithm for cone-beam reconstruction with a circular-scanning locus [5]. Using the same approach, a generalized Feldkamp algorithm for equispacial cone-beam data was derived based on a derivative-free, equispacial fan-beam reconstruction formula for a non-circular scanning locus. In the generalized Feldkamp reconstruction, cone-beam projection data from different orientations are filtered and back-projected along X-ray paths after voxel-to-source distance and angular differential are properly modified. The reconstructed value of a voxel is the sum of contributions from all horizontally tilted fan-beams passing through that voxel. The key formulas are briefly reviewed in this section, as a background for the derivation of a generalized Feldkamp formula for equiangular cone-beam projection data.

As shown in Fig. 1, the equispacial fan-beam reconstruction formula for a non-circular scanning locus is expressed as [7]:

$$g(x, y) = \frac{1}{2} \int_0^{2\pi} \frac{\rho^2(\beta)}{[\rho(\beta) - s]^2} \int_{-\infty}^{\infty} R(p, \beta) f \left[\frac{\rho(\beta)t}{\rho(\beta) - s} - p \right] \frac{\rho(\beta)}{\sqrt{\rho^2(\beta) + p^2}} dp d\beta, \quad (1)$$

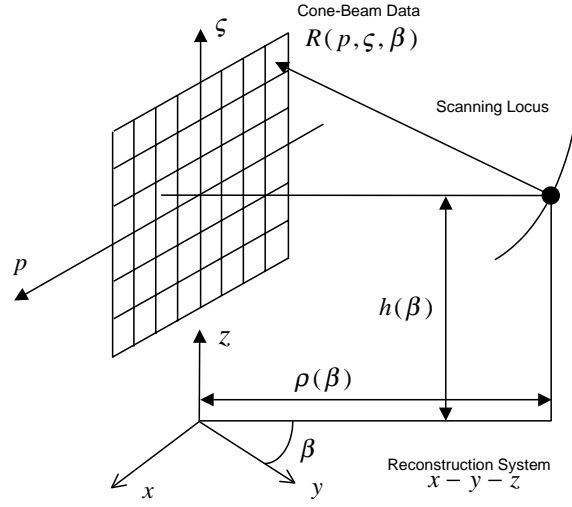


Fig. 2. Geometry of equispacial cone-beam reconstruction.

where $g(x, y)$ is the reconstructed image, $\rho(\beta)$ is the distance from the X-ray source to the origin of the reconstruction system, $R(p, \beta)$ fan-beam projection data as a function of the detector linear position p and the X-ray source rotation angle β , f the reconstruction filter, and

$$t = x \cos \beta + y \sin \beta$$

$$s = -x \sin \beta + y \cos \beta.$$

As shown in Fig. 2, the generalized Feldkamp algorithm for equispacial cone-beam data is formulated as [8]:

$$g(x, y, z) = \frac{1}{2} \int_0^{2\pi} \frac{\rho^2(\beta)}{[\rho(\beta) - s]^2} \int_{-\infty}^{\infty} R(p, \varsigma, \beta) f \left[\frac{\rho(\beta)t}{\rho(\beta) - s} - p \right] \frac{\rho(\beta)}{\sqrt{\rho^2(\beta) + p^2 + \varsigma^2}} dp d\beta, \quad (2)$$

where $g(x, y, z)$ is the reconstructed image, $\rho(\beta)$ is the distance from the X-ray source to the z axis of the reconstruction system, $R(p, \varsigma, \beta)$ cone-beam projection data as a function of the detector spatial position (p, ς) and the X-ray source rotation angle β , f the reconstruction filter, and

$$t = x \cos \beta + y \sin \beta$$

$$s = -x \sin \beta + y \cos \beta.$$

$$\varsigma = \frac{\rho(\beta)[z - h(\beta)]}{\rho(\beta) - s}$$

3. Generalized Feldkamp reconstruction in the equiangular case

The essential step in the generalized Feldkamp reconstruction described in the preceding section may be considered as appropriate correction from cone-beam data to fan-beam data, so that exact fan-beam reconstruction of a 3D impulse function can be achieved in the transaxial plane containing the impulse. The correction is done by multiplying cone-beam data with the cosine of the X-ray tilting angle. In other

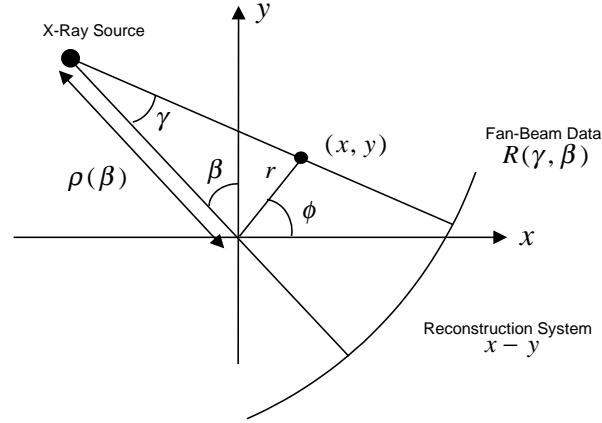


Fig. 3. Geometry of equiangular fan-beam reconstruction.

words, the generalized Feldkamp reconstruction can be decomposed into two steps: (1) cone-beam to fan-beam data conversion, and (2) fan-beam reconstruction.

Recently, we derived and tested the derivative-free equiangular fan-beam reconstruction formula for non-circular scanning loci. The new formula is the same as the conventional equiangular fan-beam formula, except that the constant source-to-origin distance is made a function with respect to the X-ray source rotation angle [9]:

$$g(x, y) = \frac{1}{2} \int_0^{2\pi} \int_{-\infty}^{\infty} R(\gamma, \beta) f[r \cos(\beta + \gamma - \phi) - \rho(\beta) \sin \gamma] \rho(\beta) \cos \gamma d\gamma d\beta, \quad (3)$$

where $g(x, y)$ is the reconstructed image, as shown in Fig. 3, $\rho(\beta)$ is the distance from the X-ray source to the origin of the reconstruction system, $R(\gamma, \beta)$ fan-beam projection data as a function of the detector angular position γ and the X-ray source rotation angle β , f the reconstruction filter, and

$$r = \sqrt{x^2 + y^2}$$

$$\phi = \tan^{-1} \frac{x}{y}.$$

In order to derive a generalized Feldkamp image reconstruction formula for equiangular cone-beam data, we applying the fan-beam reconstruction Eq. (3) with cosine-corrected cone-beam data collected from a 3D-scanning locus, we obtain the main result of this paper:

$$g(x, y, z) = \frac{1}{2} \int_0^{2\pi} \int_{-\infty}^{\infty} R(\gamma, \varsigma, \beta) f[r \cos(\beta + \gamma - \phi) - \rho(\beta) \sin \gamma] \rho(\beta) \cos \gamma \cos \tau d\gamma d\beta, \quad (4)$$

where, as shown in Fig. 4, $g(x, y, z)$ is the reconstructed image, $\rho(\beta)$ is the distance from the X-ray source to the z axis of the reconstruction system, $R(\gamma, \varsigma, \beta)$ cone-beam projection data as a function of the detector angular position (γ, ς) and the X-ray source rotation angle β , f the reconstruction filter, and

$$r = \sqrt{x^2 + y^2}$$

$$\phi = \tan^{-1} \frac{x}{y}$$

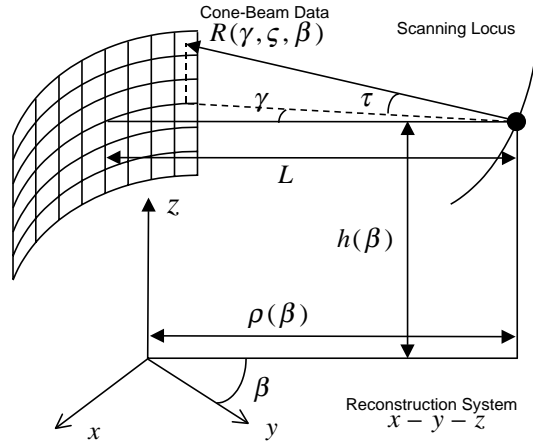


Fig. 4. Geometry of equiangular cone-beam reconstruction.

Table 1
Parameters of the 3D Shepp and Logan head phantom used in the simulation

No.	x	y	z	a	b	c	α	μ
1	0	0	0	0.69	0.92	0.9	0	2
2	0	0	0	0.6624	0.874	0.88	0	-0.98
3	-0.22	0	-0.25	0.41	0.16	0.21	108	-0.02
4	0.22	0	-0.25	0.31	0.11	0.22	72	0.02
5	0	0.35	-0.25	0.21	0.25	0.5	0	0.02
6	0	0.1	-0.25	0.046	0.046	0.046	0	0.02
7	-0.08	-0.65	-0.25	0.046	0.023	0.02	0	0.01
8	0.06	-0.65	-0.25	0.046	0.023	0.02	90	0.01
9	0.06	-0.105	0.625	0.056	0.04	0.1	90	0.02
10	0	0.1	0.625	0.056	0.056	0.1	0	-0.02

$$\tau = \tan^{-1} \frac{\varsigma}{L}$$

$$\varsigma = \frac{\rho(\beta)[z - h(\beta)]}{\rho(\beta) - s}$$

$$s = -x \sin \beta + y \cos \beta$$

Note that data $R(\gamma, \varsigma, \beta)$ are distributed on a segment of the cylindrical surface of radius L .

4. Numerical simulation

A 3D version of Shepp and Logan head phantom was used in the simulation. In order to obtain the 3D head phantom, the 2D ellipses of the conventional head phantom were made ellipsoids and repositioned within an imaginary skull. The head phantom parameters are listed in Table 1, where there are ten ellipsoids, x, y, z denote the center of an ellipsoids, a, b, c are the x, y, z semi-axes respectively, α is the rotation angle of an ellipsoid (about the z axis), and μ is a relative X-ray attenuation coefficient. The effective X-ray attenuation coefficient at a point is the sum of the relative parameters of ellipsoids containing that point.

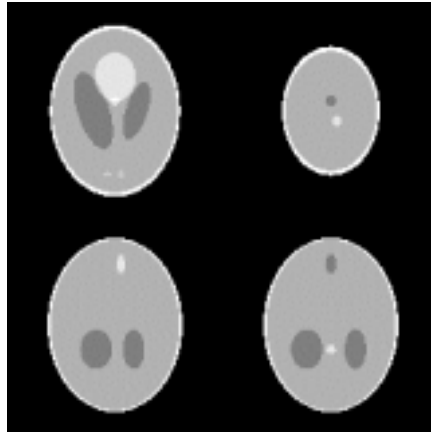


Fig. 5. Four slices of Shepp and Logan's three-dimensional head phantom at $z = -0.25$ (upper-left), $z = 0.625$ (upper-right), $y = -0.105$ (lower-left) and $y = 0.1$ (lower-right), respectively.

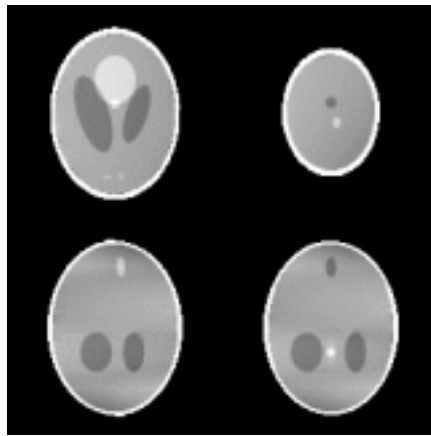


Fig. 6. Four reconstructed slices obtained using a helical cone-beam reconstruction algorithm with equiangular data, for scanning radius of 3 and helical pitch of 1.25, corresponding to the four slices of the phantom shown previously.

Figure 5 shows four slices of the 3D Shepp and Logan head phantom. Two are horizontal slices with $z = -0.25$ (upper-left) and $z = 0.625$ (upper-right). The other two are vertical slices with $y = -0.105$ (lower-left) and $y = 0.1$ (lower-right). Note that the real gray level was transformed according to a linear relationship for better visualization. This transformation linearly maps the interval $[0.95, 1.05]$ into 256 discrete gray levels. Truncation was done when necessary.

In the numerical simulation, the detector plane is 2.2 by 2.2 with 128 by 128 pixels and is so placed for the ease of computation that its vertical axis is the z -axis. One hundred projection images with a 3.6-degree angular interval were used for reconstruction. In order to handle patients or rod-shaped specimens, a helical scanning reconstruction algorithm can be designed to handle equiangular cone-beam data according to the equiangular data Feldkamp-type formula derived in the proceeding section. Contrast to Feldkamp's algorithm where the scanning locus of an X-ray source is a circle, the helical cone-beam reconstruction algorithm requires the translation of the X-ray source and the simultaneous rotation of the specimen to produce a helical scanning locus in the reconstruction coordinate system. For any horizontal slice to be reconstructed, it is assumed that such a helical turn can always be found

that the turn is divided by the concerned slice into upper-and lower-halves. Projection images collected from this turn are used to reconstruct the slice. Figure 6 shows four reconstructed images obtained using the equal-angular helical cone-beam reconstruction algorithm, with scanning radius 3 and helical pitch 1.25. Note that the simulation conditions and parameters are identical to those that were used to test the generalized Feldkamp-type formula with a helical scanning locus [8]. As expected, the image quality of cone-beam reconstruction with equiangular data is in excellent agreement with the counterparts with equispacial data, the corresponding differences between the relative errors of the representative slices being less than 1%.

5. Discussion and conclusion

Although the generalized Feldkamp formula with equiangular cone-beam data is still approximate, several analytic properties of the formula can be established regarding exactness in reconstruction, similar to what was done for Feldkamp reconstruction with equispacial data. First, the generalized Feldkamp reconstruction is exact on the mid-plane. In the 2D case, the generalized Feldkamp algorithm degrades to the derivative-free non-circular fan-beam reconstruction formula. Under some moderate conditions about the scanning locus, reconstruction must be exact [7,9]. Second, the generalized Feldkamp reconstruction produces exact vertical integrals. The longitudinal integral of the spatially varying point spread function of the generalized cone-beam algorithm is a 2D impulse function. As a result, after longitudinal integral, an exact 2D parallel projection can be synthesized. Third, the generalized Feldkamp reconstruction is exact for longitudinal homogeneous specimens. Finally, we emphasize that even if the scanning locus does not quite satisfy the conditions for exact reconstruction, the fan-beam and cone-beam formulas still produce satisfactory image quality. If it is necessary in this case, we can always obtain the above mentioned exactness properties by applying the exact fan-beam formula that contains a derivative term with respect to the locus.

In conclusion, motivated by medical cone-beam X-ray applications, we have derived a generalized Feldkamp image reconstruction formula for equiangular cone-beam projection data. In the case that projection data are in such a format, our formula can be used to reconstruct the image without interpolation induced blurring. Extension and evaluation of our equiangular cone-beam image reconstruction formula are underway for cone-beam half-scanning [10] and multi-source geometry [11].

Acknowledgment

The research is sponsored in part by the NIH R01 70209 (PI: Hong Liu), Whitaker Foundation Biomedical Engineering Grant RG-98-0448 (PI: Shiyong Zhao), and NIH R01 03590 (PI: Ge Wang).

References

- [1] K. Taguchi and H. Aradate, Algorithm for image reconstruction in multi-slice helical CT, *Med. Phys.* **25** (1998), 550–561.
- [2] H. Hu, Multi-slice helical CT: scan and reconstruction, *Med. Phys.* **26** (1999), 5–18.
- [3] C. Axelsson and P.E. Danielsson, Three-dimensional reconstruction from cone-beam data in $o(n^3 \log n)$ time, *Phys. Med. Biol.* **39** (1994), 477–491.
- [4] H. Kodo, F. Noo and M. Defrise, Cone-beam filtered-backprojection algorithm for truncated helical data, *Phys. Med. Biol.* **43** (1998), 2885–2909.
- [5] L.A. Feldkamp, L.C. Davis and J.W. Kress, Practical cone-beam algorithm, *J. Opt. Soc. Am.* **1**(A) (1984), 612–619.

- [6] G.T. Gullberg and G.L. Zeng, A cone-beam filtered backprojection reconstruction algorithm for cardiac single photon emission computed tomography, *IEEE Trans. Medical Imaging* **11** (1992), 91–101.
- [7] G. Wang, T.H. Lin and P.C. Cheng, A derivative-free non-circular fan-beam reconstruction formula, *IEEE Trans. on Image Processing* **2** (1993), 543–547.
- [8] G. Wang, T.H. Lin, P.C. Cheng and D.M. Shinozaki, A General Cone-Beam Reconstruction Algorithm, *IEEE Trans. on Medical Imaging* **12**(3) (1993), 486–495.
- [9] K. Redford, G. Wang and M.W. Vannier, Equiangular fan-beam CT reconstruction for a non-circular scanning locus, *Optical Engineering* **38** (1999), 1335–1339.
- [10] G. Wang, Y. Liu, T.H. Lin and P.C. Cheng, A half-scan cone-beam x-ray microtomography formula, *Journal of Scanning Microscopy* **16** (1994), 216–220.
- [11] Y. Liu, H. Liu, Y. Wang and G. Wang, Half-scan cone-beam CT fluoroscopy with multiple X-ray sources, *Medical Physics* **28** (2001), 1466–1471.